Journal of Power Sources 273 (2015) 162–167

Contents lists available at ScienceDirect

Journal of Power Sources

journal homepage: www.elsevier.com/locate/jpowsour

Lithium–sulphur battery with activated carbon cloth-sulphur cathode and ionic liquid as electrolyte

Agnieszka Swiderska-Mocek*, Ewelina Rudnicka

Faculty of Chemical Technology, Poznan University of Technology, PL-60 965 Poznan, Poland

HIGHLIGHTS

- A binder-free activated carbon cloth-sulphur (ACC-S) cathode was prepared.
- The ACC-S cathode has good performance with an ionic liquid electrolyte.
- The ACC-S/Li cell shows a relatively high capacity of 830 mAh g^{-1} after 50 cycles.

ARTICLE INFO

Article history:
Received 20 May 2014
Received in revised form
25 August 2014
Accepted 3 September 2014
Available online 16 September 2014

Keywords:
Activated carbon cloth-sulphur cathode
Sulphur cathode
Ionic liquid
Lithium–sulphur battery

ABSTRACT

In this study a binder-free activated carbon cloth-sulphur (ACC-S) composite cathode is presented. Such a cathode was obtained using the impregnating technique of microporous activated carbon cloth with elemental melted sulphur. The surface morphology of an activated carbon cloth-sulphur electrode was studied using a scanning electron microscope (SEM), which was equipped with an EDX spectroscopy attachment. Electrochemical properties of the ACC-S composite cathode was tested in an ionic liquid electrolyte consisting of 1-ethyl-3-methylimidazolium bis(trifluoromethanesulphonyl)imide ($EtMeImNTf_2$) and bis(trifluoromethanesulphonyl)imide ($LiNTf_2$). The ACC-sulphur cathode working together with lithium anode was tested with the use of cyclic voltammetry (CV), galvanostatic charge/discharge cycles and electrochemical impedance spectroscopy (EIS). The capacity and cyclic stability of the ACC-S composite cathode were much better than those for the sulphur cathode (a mixture of sulphur from graphene nanoplatelets and carbon black) tested in the same ionic liquid electrolyte. The ACC-sulphur cathode showed good cyclability and coulombic efficiency (99%) with the ionic liquid electrolyte. The reversible capacity of the ACC-S|electrolyte|Li cell was ca. 830 mAh g^{-1} after 50 cycles.

1. Introduction

The lithium–sulphur (Li–S) battery is a promising electrochemical energy storage system that has a high theoretical specific capacity of 1675 mAh g^{-1} and a theoretical energy density of 2600 Wh kg^{-1}, which is 3–5 times that of Li-ion batteries [1–3]. Interest in these batteries has been observed in recent years. Replacement of the traditional insertion cathodes ($LiCoO_2$, $LiFePO_4$) with sulphur has many advantages, such as e.g. a low operating voltage (2.15 V vs. Li^+/Li), which increases their safety [4]. Sulphur is also an attractive material because of its large reserves, low-cost and being environmentally friendly when compared with certain toxic transition-metal compounds. The most stable allotrope of sulphur at room temperature is octa-sulphur (cyclo-S_8). It reacts reversibly with metallic lithium:

$$S_8 + 16Li^+ + 16e^- \leftrightarrow 8Li_2S \quad (1)$$

Despite the many advantages of the above-mentioned Li–S cell, there may also be certain disadvantages. The biggest problem is connected with solubility of long chain polysulfides (PS) formed at the cathode by reduction of pure sulphur (S_8) and/or by oxidation of short chain polysulfides. The intermediate discharge products (Li_2S_x, $2 < x < 8$) are a result of this high solubility, which leads to the reduction of sulphur active mass [5]. Another problem is the insulating nature of sulphur. Therefore, additives are needed to increase electronic conductivity of the cathode. All changes and modifications of the Li–S batteries are designed to improve stability of the electrode structure and the utilization efficiency of sulphur in the cathode. This can be mostly achieved by a

* Corresponding author.
E-mail address: agnieszka.swiderska-mocek@put.poznan.pl (A. Swiderska-Mocek).

http://dx.doi.org/10.1016/j.jpowsour.2014.09.020
0378-7753/

modification of the sulphur-based composite cathode material and by selecting the most suitable electrolytes.

Sulphur–carbon-based composites are more attractive because, encapsulation of sulphur in carbon improves its utility as an active mass and prevents diffusion of polysufides to the electrolyte solution. This reduces the phenomenon, which significantly limits the capacity of sulphur cathodes [3,6]. For this purpose mesoporous carbon [7], carbon nanotubes [8,9], activated carbon [10] and graphene [11,12] were used. Sulphur–carbon composites were synthesized by various methods. Ball-milling or mixing sulphur powder and carbon materials have been used in conventional sulphur electrodes [3]. There are other methods applied for the preparation of the electrodes (binder-free cathodes), in which sulphur is injected into the pores of carbon fibres [10] or sulphur atoms are deposited on multiwalled carbon nanotubes [8,9]. Manipulation of the pore size (mesoporous vs. microporous) and structure of carbon materials (graphene, nanotubes, and carbon hybrids) can further improve the electrochemical performance of Li–S batteries.

In the case of Li-sulphur batteries solubility of polysulfides in the electrolyte is not inevitable. Therefore, for long-term stability we need to properly understand the influence of PS dissolution and PS reactivity in different electrolytes [4,13,14]. The use of an electrolyte based on ionic liquid (IL) can contribute to the suppression of solubility of polysulfides. In addition, it also increases system safety and this is due to the fact that ionic liquids are characterized by negligible vapour pressure and are completely non-volatile [15]. They additionally have considerable thermal stability, a wide liquid-phase range, a broad electrochemical stability and they exhibit high conductivity [16,17]. These features encourage the use of ionic liquids as electrolytes in Li–S batteries. Among ILs, those based on 1-ethyl-3-methylimidazolium [$EtMeIm^+$], N-butyl-N-methylpyrrolidinium [$BuMePyr^+$] and N-butyl-N-methylpiperidinium [$BuMePip^+$] cations and the bis(trifluoromethanesulphonyl)imide anion, [NTf_2] were tested as solvents for lithium salts in Li–S batteries [18–22].

A common problem in the practical application of the lithium battery is to use a lithium metal anode. Lithium metal used as anode material has numerous advantages, such as a high theoretical specific capacity of 3860 mAh g^{-1} and very low density (0.535 g cm^{-3}). The main problem, however, is its high reactivity, which during a prolonged operation of the cell (cyclic deposition and dissolution of Li) leads to the formation of dendrites on the metal surface, causing serious problems with safety and efficiency of the system. Therefore, attempts were made to replace the lithium anode with carbon anodes, mainly graphite [23,24].

In this study we prepared binder-free sulphur–carbon composite cathodes using the impregnating technique of microporous activated carbon cloth with elemental melted sulphur (ACC-S). Thus, the produced carbon cloth/sulphur cathodes have demonstrated very good electrochemical performance. These electrodes were tested in the system with a lithium anode in the electrolyte based ionic liquid – 1-ethyl-3-methylimidazolium bis(trifluoromethanesulphonyl)imide ($EtMeImNTf_2$).

2. Experimental

2.1. Materials

Elemental sulphur (purum >99.5%, Aldrich), activated carbon cloth (ACC, specific surface: 2485 m^2 g^{-1}, average particle size: 1.67 nm, the microporous structure of carbon cloth, Kynol®), lithium foil (0.75 mm thick, Aldrich), single layer graphene (G, specific surface: 570 m^2 g^{-1}, ACS Material, USA), graphene nanoplatelets (GN, thickness 2–10 nm, ACS Material, USA), carbon black (CB, Alfa Aesar), poly(vinylidene fluoride) (PVdF, Fluka), N-methyl-2-pyrrolidinone (NMP, Fluka), acetone (POCh, Poland), dimethyl carbonate (DMC, Aldrich), lithium bis(trifluoromethanesulfonyl) imide ($LiNTf_2$, Fluka) and 1-ethyl-3-methylimidazolium bis(trifluoromethanesulphonyl)imide ($EtMeImNTf_2$, Aldrich) were used as received.

Liquid electrolyte (1 M $LiNTf_2$ in $EtMeImNTf_2$) was obtained by dissolution of solid $LiNTf_2$ salt in liquid $EtMeImNTf_2$ at room temperature in a dry argon atmosphere in a glove box. The water content in electrolytes, analysed with a standard Karl–Fisher titrant (Aldrich), was below 50 ppm.

A round-shaped lithium electrode was cut off from metallic-lithium foil (Aldrich, 0.75 mm thick) and was used as the counter electrode (anode).

2.2. Carbon/sulphur and sulphur cathode preparation

The carbon/sulphur cathode was prepared by impregnating microporous activated carbon cloth with elemental melted sulphur (ACC-S). Elemental sulphur was placed on the bottom of a stainless steel vessel and was suspended on an activated carbon cloth. Upon closing the vessel, it was heated at 160–180 °C for 5 h. The sulphur content in the activated carbon cloth was monitored by weight (weight of the carbon cloth before and after impregnation of sulphur). Discs with an area of 0.785 m^2 and a sulphur content of 1 mg were then cut from the cloth. The volumetric capacity of the carbon/sulphur cathode is very small. This parameter is important from the point of view of suitability of the electrode to some practical applications. Also, an electrode must show good performance at a sufficiently high mass loading, or high capacity loading, which are measurements of electrode mass per unit area (mg cm^{-2}) and electrode capacity per unit area (mAh cm^{-2}). Electrodes in commercial cells commonly show capacity loadings of 2.5–3.5 mAh cm^{-2}. In this case, the capacity of the sulphur electrode was 2.12 mAh cm^{-2}.

Before electrochemical testing the carbon/sulphur cathode was rubbed with a mixture of nanoplatelets and PVdF suspended in acetone. After evaporation of acetone the ratio of components was (S):(GN):(PVdF) = 80:10:10 (by weight).

The sulphur cathode was prepared on aluminium foil using the casting technique, from a slurry of elemental sulphur (S), graphene nanoplatelets (GN), carbon black (CB) and PVdF in NMP. The ratio of components was (S):(GN):(CB):(PVdF) = 60:20:10:10 (by weight). The layer of the sulphur electrode was formed by vacuum evaporation of the solvent (NMP).

2.3. Measurements

Cells were assembled in a dry argon atmosphere in a glove box. Electrodes were separated by a glass micro-fibre GF/A separator (Whatman) soaked with the electrolyte and placed in an adapted 0.5″ Swagelok® connecting tube.

The morphology of activated carbon cloth and carbon/sulphur (ACC-S) cathodes (pristine and after electrochemical cycling) was observed under a scanning microscope (SEM, Tescan Vega 5153), which was equipped with an EDX spectroscopy attachment. After electrochemical measurements, cells were disassembled, and electrodes washed with DMC and dried in vacuum at room temperature. All operations were made in a dry argon atmosphere in a glove box.

The electrochemical characteristic of ACC-S/1 M $LiNTf_2$ in $EtMeImNTf_2$/Li and ACC-S-Li/1 M $LiNTf_2$ in $EtMeImNTf_2$/G cells was investigated using cyclic voltammetry (CV), galvanostatic charge/discharge tests and electrochemical impedance spectroscopy (EIS). Cyclic voltammetry as well as electrochemical impedance spectroscopy (EIS) were performed with the use of the G750

Potentiostat/Galvanostat Measurements System (Gamry, USA). Cyclic voltammetry of the ACC-S cathode measurement was carried out in the potential range of 1.4–2.9 V vs. Li/Li^+ with the scan rate of 0.1 mV s^{-1}. Cycling measurements were taken with the use of the ATLAS 0461 MBI multichannel electrochemical system (Atlas-Solich, Poland) at 100 mAh g^{-1} current density. Constant current charging/discharging cycles for ACC-S/1 M $LiNTf_2$ in $EtMeImNTf_2$/Li and S/1 M $LiNTf_2$ in $EtMeImNTf_2$/Li cell were conducted between 1.2 and 2.8 V vs. the lithium reference. Impedance spectra were obtained using a frequency response analyser at a frequency range of 100 kHz–10 mHz at the open circuit potential and amplitude of 10 mV.

3. Results and discussion

Scanning electron microscopy (SEM) images of the activated carbon cloth (ACC) and the ACC-sulphur composite cathode and the corresponding energy-dispersive X-ray spectrometry (EDS) C, O and S maps are displayed in Fig. 1. The elemental mapping images of S in Fig. 1b, d and f show that they uniformly deposit sulphur on carbon fibres, as well as penetrate into their interior. As it was observed, carbon fibres are 10 μm in diameter and their morphology does not change after sulphur impregnation.

Cyclic voltammograms of the ACC-S electrode in ionic liquid (1 M $LiNTf_2$ in $EtMeImNTf_2$) are shown in Fig. 2. As it can be seen in this figure, the oxidation, broad peak was observed at the potential of ca. 2.5 V, while the reduction, broad peak at the potential of ca. 2.1 V. In this case, we only see one pair of redox peaks. In contrast, sulphur in organic solvents is most often observed in two pairs of distinct oxidation and reduction peaks at two potential regions of 2.5–2.4 and 2.3–1.8 V, respectively. Peaks at the potential region of 2.5–2.4 V can be attributed to oxidation of Li_2S and Li_2S_2 to Li_2S_8. In the case of the reduction process one peak was observed at a higher potential and it was related to the open ring reduction of cyclic S_8 to the long chain lithium polysulfides, while the other peak was observed at a lower potential, which corresponds to the reduction process of polysulfides to Li_2S_2 and Li_2S [18,25,26]. Quite differently, the discharge curve of Li/S cells using 1 M $LiNTf_2$ in $EtMeImNTf_2$ electrolyte and sulphur, which has been deposited on activated carbon cloth (the ACC-sulphur composite cathode) only shows a

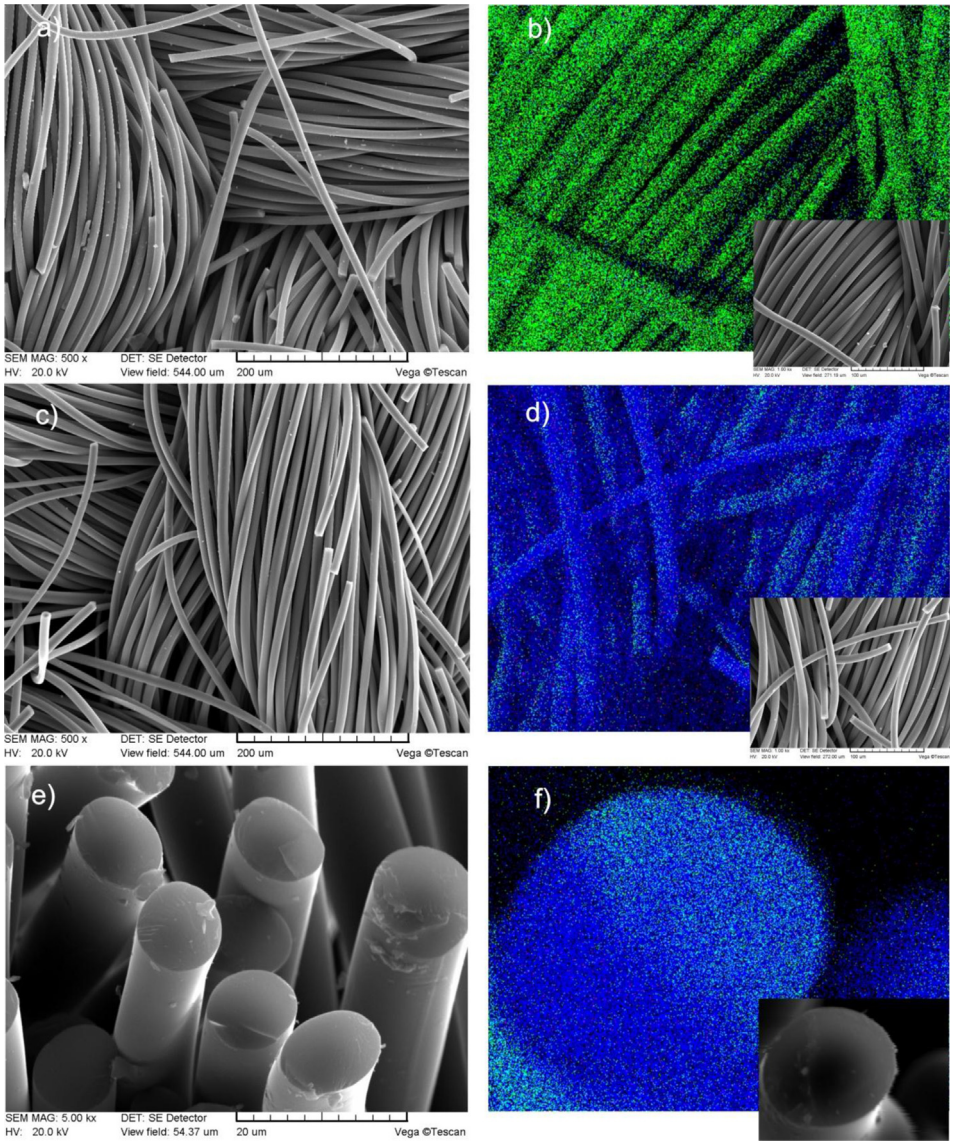

Fig. 1. SEM images obtained from the activated carbon cloth (ACC) (a, b) and ACC-S composite cathode (c, d, e and f) with corresponding EDS maps for S (blue), C (green), O (red) (b), (d) and (f). (For interpretation of the references to colour in this figure legend, the reader is referred to the web version of this article.)

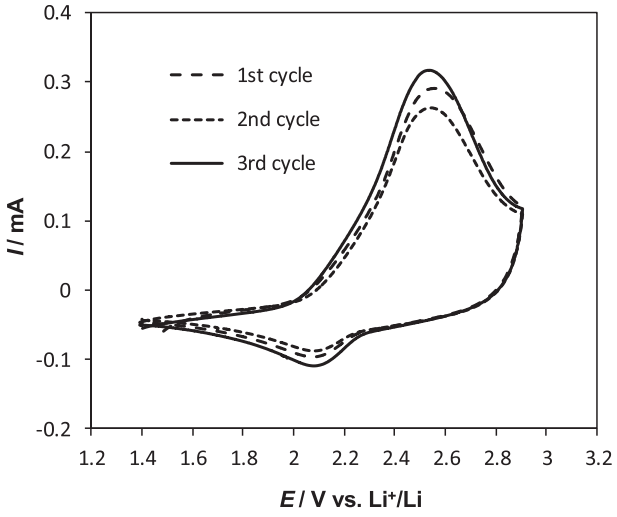

Fig. 2. Cyclic voltammogram of ACC-S cathode with 1 M $LiNTf_2$ in $EtMeImNTf_2$ vs. Li/Li^+. Scan rate: 0.1 mV s^{-1}.

single discharge plateau with an average voltage around 2.1 V, as presented in Fig. 3. For comparison, this also shows the discharge curve of the sulphur cathode obtained by mixing elemental sulphur with carbon materials (graphene nanoplatelets and carbon black). In this case the discharge curve shows two plateaus, which could be associated with the two step reaction of sulphur with lithium during the discharge process, as demonstrated in the CV measurements (Fig. 2). This difference is probably due to the fact that encapsulation of sulphur in carbon prevents the diffusion of polysufides to the electrolyte solution, leading to a continuous discharge of sulphur to Li_2S through a fast reduction of intermediate polysulfides. The same phenomenon is observed when using N-methyl-N-butyl-piperidinium bis(trifluoromethanesulfonyl) imide ionic liquid as the electrolyte [18]. The presence and position of these peaks shows the electrochemical activity and reversibility of sulphur in the ACC-sulphur composite cathode in 1 M $LiNTf_2$ in $EtMeImNTf_2$ electrolyte.

Fig. 4 shows the galvanostatic voltage profile of the charge/discharge process and coulombic efficiency of the ACC-sulphur cathode with 1 M $LiNTf_2$ in $EtMeImNTf_2$ electrolyte, at a current rate of 0.06 C (100 mAh g^{-1} based on sulphur). The capacity of the discharging and charging processes at the first cycle was 1668 and 1514 mAh g^{-1}, respectively, resulting in a coulombic efficiency of 91%. In subsequent cycles, coulombic efficiency increased to almost 99–100%. In turn, during the next cycles the capacity of the ACC-sulphur electrode decreased slightly to stabilize at ca. 1270 mAh g^{-1} after 10 cycles. After 50 cycles, the reversible capacity reached a value of 830 mAh g^{-1} and was 50% of the theoretical capacity (ca. 1670 mAh g^{-1}). It can be seen that the modified sulphur electrode provides good results in the system with the electrolyte ionic liquid. However, still a significant loss of capacity is observed. It results from the solubility of polysulfides, which affect the performance of the cathode, but also from the presence of the anode in the form of lithium metal. The reactivity of lithium metal with the ionic liquid leads to changes on its surface (including those unfavourable, i.e. dendrite formation) resulting in reduced efficiency of the entire system. Slightly worse results were obtained for the S–C (sulphur coated mesoporous carbon composites)/Li cell with the ionic liquid electrolyte. S–C/Li cells using the $EtMeImNTf_2$ ionic liquid have demonstrated that the sulphur cathode can achieve a reversible capacity of ca. 600 mAh g^{-1}, corresponding to a 36% utilization of sulphur [20]. If you use N-methyl-N-butyl-piperidinium bis(trifluoromethanesulfonyl) imide ionic liquid as the electrolyte, we obtain a reversible capacity of 750 mAh g^{-1} for the S–C/Li cell [18]. The use of the binder free electrode containing only carbon nanotubes and sulphur in combination with the N-methyl-N-butyl-pyrrolidinium bis(trifluoromethanesulfonyl) imide ionic liquid provides a high value of the volumetric energy density at low gravimetric energy densities (the loads of sulphur per cm^2 electrode are much higher than in slurry composed electrodes) [27]. For comparison, Fig. 5 shows the charge and discharge capacity and efficiency of the S/1 M $LiNTf_2$ in $EtMeImNTf_2$/Li cell, cycled at a

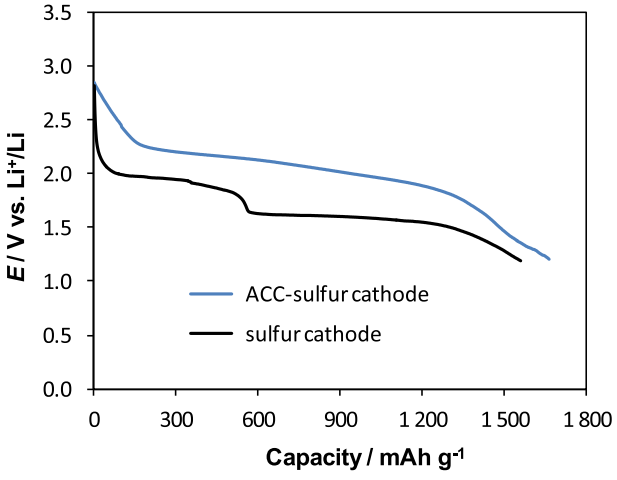

Fig. 3. The initial discharge profiles for the ACC-sulphur composite and sulphur cathodes in 1 M $LiNTf_2$ in $EtMeImNTf_2$ electrolyte at a rate of 0.06 C (100 mAh g^{-1}) in the voltage range of 1.2–2.8 V (vs. Li^+/Li).

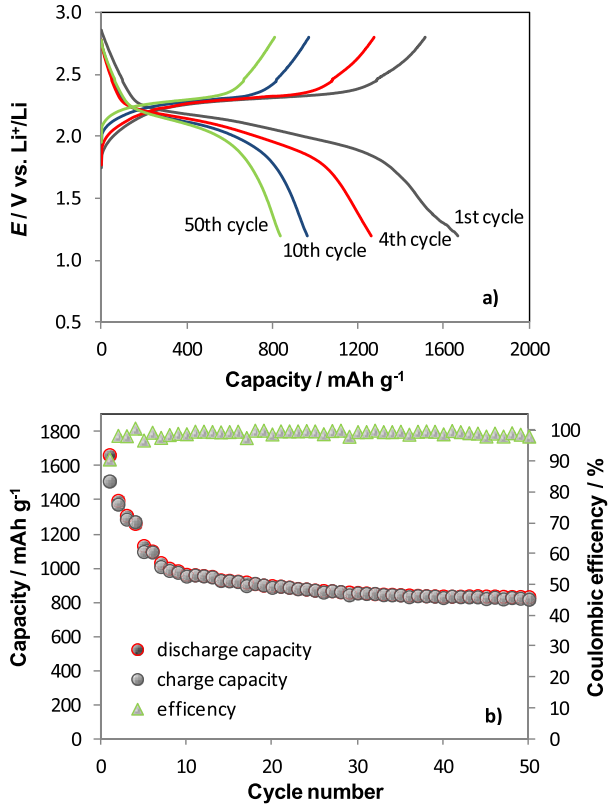

Fig. 4. Galvanostatic charge/discharge profile (a) and charge–discharge capacity of the ACC-S/1 M $LiNTf_2$ in $EtMeImNTf_2$/Li cell at 100 mAh g^{-1} with coulombic efficiency (b).

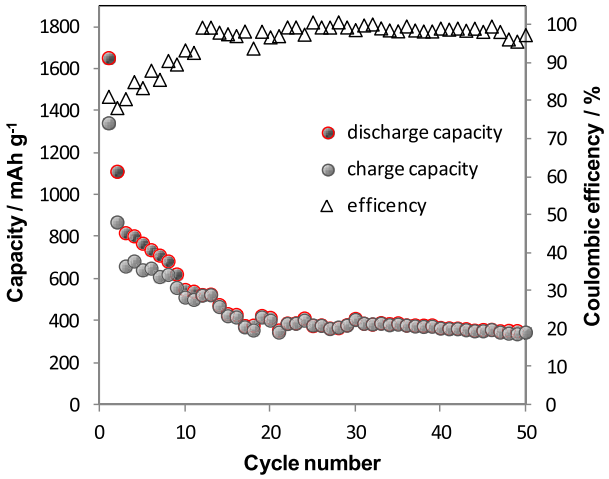

Fig. 5. Charge–discharge capacity and coulombic efficiency of the S/1 M $LiNTf_2$ in $EtMeImNTf_2$/Li at 100 mAh g^{-1}.

constant current of 100 mAh g^{-1}. After the first fifteen cycles the reversible capacity of the composite S cathode (a mixture of sulphur from graphene nanoplatelets and carbon black) drops from the initial 1650 to 370 mAh g^{-1}, and then remains steady at ca. 350 mAh g^{-1} at the following cycles. This value is more than two times lower than that of the activated carbon cloth-sulphur cathode. This data seems to indicate that the use of the ACC-sulphur electrode may not only improve the capacity utilization, but also cycling stability of the lithium–sulphur battery. It should also be noted that the density of the electrode (ACC-sulphur and sulphur) has an impact on system performance. A decrease in the density of the electrode, in this case, the use of ACC-sulphur cell, results in an increase of cell efficiency.

The observed significant loss of capacity in the first few cycles may, in fact, be associated with the formation of the passivation layer on the electrode surface. Fig. 6 shows scanning electron microscopy (SEM) images and EDX spectrum of a pristine ACC-sulphur cathode and those after electrochemical cycling. Galvanostatic charging/discharging of the electrode material leads to changes on the surface. Also, the EDX analysis suggests changes and shows the presence of an additional element on the electrode surface (fluorine probably originating from electrochemical decomposition of the NTf_2 anion). It should be added here that the analysis of the SEI layer is difficult and requires high precision. This is mainly the result of considerable dynamics of changes in the SEI layer that occur during electrochemical processes. Changes in the structure of the SEI layer may also arise in the preparation of the sample for analysis. The biggest problem is to separate the SEI layer (if necessary) from the surface of the electrode. The presence of the electrolyte or the residual solvent after washing of the SEI layer may influence a change in the original appearance of the layer. After separation and washing, there is still the problem of isolation. Most of the SEI components are highly sensitive to contamination, air and humidity. Therefore, the components of the SEI layer may be changed or modified during the initial preparation of the sample for analysis. Therefore, all procedures (from preparation to analysis) have to be carried out under an inert atmosphere (the glove box) [28,29]. The technique applied in this experiment (SEM) made it possible only to observe changes at the electrode surface (pristine and after the electrochemical process of charging and discharging). More accurate and comprehensive information on the structure of the SEI layer would require testing of high sequencing (images after each

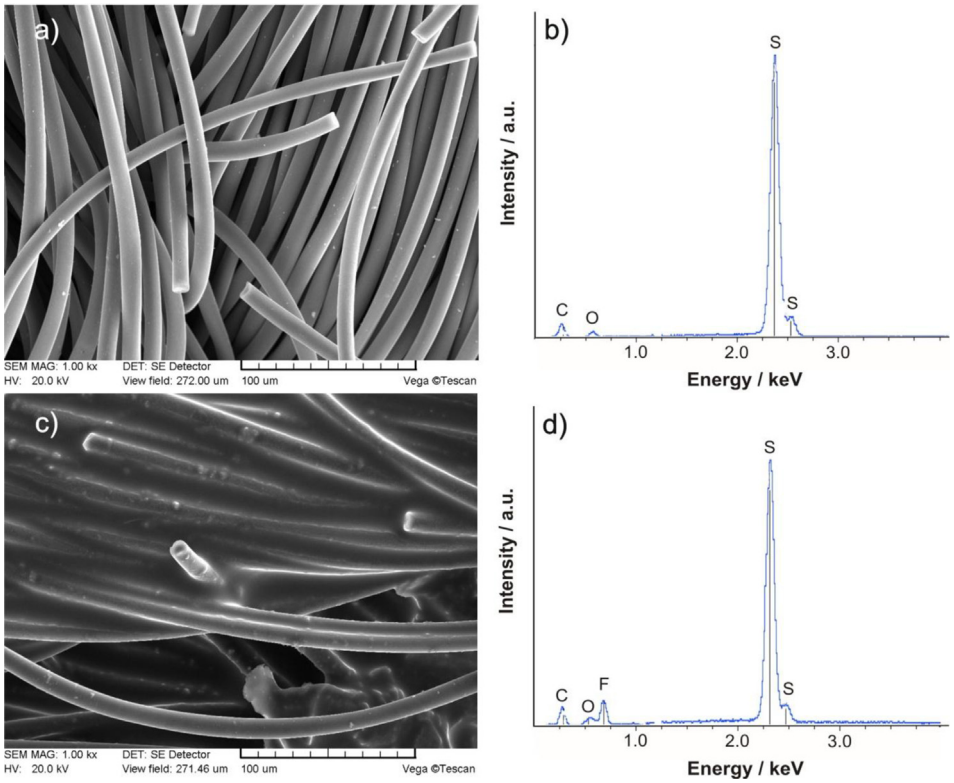

Fig. 6. SEM images and EDX spectrum of the ACC-sulphur cathode: pristine electrode (a, b) and after 50 charge/discharge cycles (c, d). Magnification: 1000×.

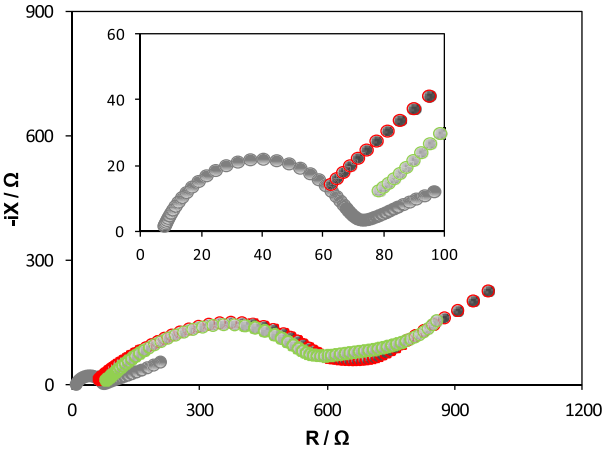

Fig. 7. Nyquist plots of ACC-sulphur cathode after assembling (grey circles), after discharge/charge/discharge at 1.44 V (red circles) and after 50 charge/discharge at 1.43 V (green circles). (For interpretation of the references to colour in this figure legend, the reader is referred to the web version of this article.)

charging and discharging) and the use of additional techniques (e.g. FTIR and Raman spectroscopy).

Changes on the surface of the cathode also provide an impedance spectrum. The EIS curves for the ACC-sulphur cathode are shown in Fig. 7 (the electrode after assembling, after discharge/charge/discharge and after 50 galvanostatic charging/discharging cycles). All the Nyquist plots included the 'flat semicircle' or two semicircles at higher frequencies and a line at lower frequencies, indicating that the electrode reactions were controlled by a mixture of the SEI layer, charge transfer and diffusion steps. The shape of the 'flat semicircle' is a result of a combination of at least two time constants *RC*, related with the SEI layer (R_{SEI}, C_{SEI}) and the charge transfer process which occurs at the double layer formed between SEI and the electrodes (R_{ct}, C_{dl}). The sloping straight line at low frequencies corresponds to the Li-ion diffusion in the bulk and represents the Warburg impedance (Z_W). The sum of electrolyte resistance (R_{el}), charge transfer resistance (R_{ct}) and surface film resistance (R_{SEI}) of the ACC-sulphur cathode after discharge/charge/discharge is ten times higher than that for the pristine electrode. Subsequent cycles do not cause significant changes and have an impedance spectrum. However, it should be noted that after 50 charge/discharge cycles, a shortened part of the spectrum is responsible for the diffusion process. This is probably related to the formation of a stable SEI layer on the surface of the ACC-sulphur electrode.

4. Conclusions

These results show that a sulphur-impregnated activated carbon cloth can serve as a promising cathode for Li–S cells. Due to its porous structure, it ensures better penetration of the electrolyte and hence a lower escape rate of sulphur reduction products. The morphology and structure of porous activated carbon cloth facilitates an increase in the load of sulphur, which can lead to an increase in the total specific capacity of the cathode. Such a composite cathode also interacts well with a non-volatile electrolyte based on $EtMeImNTf_2$ ionic liquid.

Galvanostatic charging/discharging, CV, EIS and SEM show that the lithium intercalation and deintercalation process occurs quite reversibly in ACC-sulphur materials with good cycling stability. Scanning electron microscopy (SEM) images of pristine electrodes and those taken after electrochemical cycling show changes which may be interpreted as a result of SEI formation.

Charge/discharge tests of ACC-S/1 M $LiNTf_2$ in $EtMeImNTf_2$/Li cells indicate that the initial discharge capacity is 1665 mAh g^{-1} at a current density of 100 mAh g^{-1}, and the reversible capacity can be stabilized at 830 mAh g^{-1} after 50 cycles.

All the recorded results show that the activated carbon cloth–sulphur composite cathode demonstrates a good cycle life capability in combination with lithium anode and ionic liquid electrolyte.

Acknowledgement

The support of grant no. 31-277/2014 DSPB is gratefully acknowledged.

References

[1] E. Peled, A. Gorenshtein, M. Segal, Y. Sternberg, J. Power Sources 26 (1989) 269–271.
[2] S. Evers, L.F. Nazar, Acc. Chem. Res. 46 (2013) 1135–1143.
[3] A. Manthiram, Y. Fu, Y.-S. Su, Acc. Chem. Res. 46 (2013) 1125–1134.
[4] S.S. Zhang, J. Power Sources 231 (2013) 153–162.
[5] Y.V. Mikhaylik, J.R. Akridge, J. Electrochem. Soc. 151 (2004) A1969–A1976.
[6] X. Ji, L.F. Nazar, J. Mater. Chem. 20 (2010) 9821–9826.
[7] S.R. Chen, Y.P. Zhai, G.L. Xu, Y.X. Jiang, D.Y. Zhao, J.T. Li, L. Huang, S.G. Sun, Electrochim. Acta 56 (2011) 9549–9555.
[8] S. Dorfler, M. Hagen, H. Althues, J. Tubke, S. Kaskel, M. Hoffmann, Chem. Commun. 48 (2012) 4097–4099.
[9] J. Guo, Y. Xu, C. Wang, Nano Lett. 11 (2011) 4288–4294.
[10] R. Elazari, G. Salitra, A. Garsuch, A. Panchenko, D. Aurbach, Adv. Mater. 23 (2011) 5641–5644.
[11] J.Z. Wang, L. Lu, M. Choucair, J.A. Stride, X. Xu, H.K. Liu, J. Power Sources 196 (2011) 7030–7034.
[12] H. Wang, Y. Yang, Y. Liang, J.T. Robinson, Y. Li, A. Jackson, Y. Cui, H. Dai, Nano Lett. 11 (2011) 2644–2647.
[13] J. Scheers, S. Fantini, P. Johansson, J. Power Sources 255 (2014) 204–218.
[14] S.-E. Cheon, K.-S. Ko, J.-H. Cho, S.-W. Kim, E.-Y. Chin, H.-T. Kim, J. Electrochem. Soc. 150 (2003) A800–A805.
[15] M. Armand, F. Endres, D.R. MacFarlane, H. Ohno, B. Scrosati, Nat. Mater. 8 (2009) 621–629.
[16] M. Galiński, A. Lewandowski, I. Stępniak, Electrochim. Acta 51 (2006) 5567–5580.
[17] H.L. Ngo, K. LeCompte, L. Hargens, A.B. McEwen, Thermochim. Acta 357–358 (2000) 97–102.
[18] L.X. Yuan, J.K. Feng, X.P. Ai, Y.L. Cao, S.L. Chen, H.X. Yang, Electrochem. Commun. 8 (2006) 610–614.
[19] S. Kim, Y. Jung, S.-J. Park, Electrochim. Acta 52 (2007) 2116–2122.
[20] J. Wang, S.Y. Chew, Z.W. Zhao, S. Ashraf, D. Wexler, J. Chen, S.H. Ng, S.L. Chou, H.K. Liu, Carbon 46 (2008) 229–235.
[21] Y. Yan, Y.-X. Yin, S. Xin, J. Su, Y.-G. Guo, L.-J. Wan, Electrochim. Acta 91 (2013) 58–61.
[22] J. Park, K. Ueno, N. Tachikawa, K. Dokko, M. Watanabe, J. Phys. Chem. C 117 (2013) 20531–20541.
[23] W.A. Van Schalkwijk, B. Scrosati, Advances in Lithium-ion Batteries, Kluwer Academic Publishers, 2002.
[24] B. Scrosati, J. Garche, J. Power Sources 195 (2010) 2419–2430.
[25] S.E. Cheon, K.S. Ko, J.H. Cho, S.W. Kim, E.Y. Chin, H.T. Kim, J. Electrochem. Soc. 150 (2003) A796–A799.
[26] H. Yamin, A. Gorenshtein, J. Penciner, Y. Sternberg, E. Peled, J. Electrochem. Soc. 135 (1988) 1045–1048.
[27] M. Hagen, S. Dörfler, H. Althues, J. Tübke, M.J. Hoffmann, S. Kaskel, K. Pinkwart, J. Power Sources 213 (2012) 239–248.
[28] P. Verma, P. Maire, P. Novák, Electrochim. Acta 55 (2010) 6332–6341.
[29] H. Bryngelsson, M. Stjerndahl, T. Gustafsson, K. Edström, J. Power Sources 174 (2007) 970–975.